Ain Shams Engineering Journal (2015) 6, 691–701

Ain Shams University

Ain Shams Engineering Journal

www.elsevier.com/locate/asej
www.sciencedirect.com

ENGINEERING PHYSICS AND MATHEMATICS

Analytical and numerical solution of three-dimensional channel flow in presence of a sinusoidal fluid injection and a chemical reaction

Sahin Ahmed [a,*], **Karabi Kalita** [b], **Ali J. Chamkha** [c]

[a] *Heat Transfer and Fluid Mechanics Research, Department of Mathematics, Rajiv Gandhi Central University, Rono Hills, Itanagar 783101, Arunachal Pradesh, India*
[b] *Department of Mathematics, Gauhati University, Guwahati 781014, Assam, India*
[c] *Mechanical Engineering Department, Prince Mohammad Bin Fahd University (PMU), P.O. Box 1664, Al-Khobar 31952, Kingdom of Saudi Arabia*

Received 13 June 2014; revised 5 November 2014; accepted 26 November 2014
Available online 21 January 2015

KEYWORDS

Channel flow;
Chemically reacting fluid;
Magneto-aerodynamics;
Thermo-fluid dynamics;
Sinusoidal injection velocity;
Slip condition

Abstract Modeling of three-dimensional channel flow in a chemically-reacting fluid between two long vertical parallel flat plates in the presence of a transverse magnetic field is presented. The stationary plate is subjected to a transverse sinusoidal injection velocity distribution while the uniformly moving plate is subjected to a constant suction and slip boundary conditions. Due to this type of injection velocity, the flow becomes three dimensional. Comparisons with previously published work are performed and the results are found to be in excellent agreement. An increase in the permeability/magnetic parameter is found to escalate the velocity near the plate in motion. Growing Reynolds number or magnetic parameter enhances the x-component and reduces the z-component of the skin-friction at the wall at rest. The acquired knowledge in our study can be used by designers to control MHD flow as suitable for certain applications which include laminar magneto-aerodynamics, materials processing and MHD propulsion thermo-fluid dynamics.

1. Introduction

Flows involving the simultaneous diffusion of thermal energy and chemical species have received due attention owing to their importance in geophysical and engineering applications. Geophysical applications include investigation of underground water resources, natural gas and mineral oils. Engineering applications include absorbers, humidifiers and desert coolers.

* Corresponding author. Tel.: +91 9435024242.
E-mail addresses: heat_mass@yahoo.in (S. Ahmed), kkarabi88@gmail.com (K. Kalita), achamkha@pmu.edu.sa (A.J. Chamkha).
Peer review under responsibility of Ain Shams University.

Production and hosting by Elsevier

http://dx.doi.org/10.1016/j.asej.2014.11.013

Nomenclature

U	uniform motion of the outer plate (m s^{-1})
v_0	injection velocity of the stationary plate (m s^{-1})
$\vec{q}$	velocity vector of the fluid at $(\bar{x}, \bar{y}, \bar{z})$
$\overline{T}_0$	temperature at the stationary plate
$\overline{C}_0$	molar species concentration at the stationary plate
$\overline{T}_1$	temperature at the plate in uniform motion
$\overline{C}_1$	molar species concentration at the plate in uniform motion
$\overline{T}_e$	equilibrium temperature of the fluid
$\overline{C}_e$	equilibrium molar species concentration of the fluid
$\overline{T}$	temperature of the fluid
$\overline{C}$	molar species concentration of the fluid
A	heat sink parameter
g	acceleration due to gravity (m s^{-2})
C_P	specific heat at constant pressure (J kg^{-1} K)
D	chemical molecular diffusivity (m^2 s^{-1})
Q	rate of heat absorption per unit volume per degree Kelvin
$\bar{p}$	fluid pressure (Pa)
Re	Reynolds number
Pr	Prandtl number
Sc	Schmidt number
M	Hartmann number
K	chemical reaction parameter
h	slip parameter
Gr	Grashof number for heat transfer
Gm	Grashof number for mass transfer
m	wall thermal ratio
n	wall mass ratio
B_0	magnetic field strength
d	distance between the plates

Greek symbols

β	coefficient of volume expansion (K^{-1})
$\bar{\beta}$	volumetric coefficient expansion with species concentration (K^{-1})
ε	small reference parameter (ε 1)
θ	dimensionless fluid temperature
ϕ	dimensionless species concentration of the fluid
κ	thermal conductivity (W m^{-1} K^{-1})
ν	kinematic viscosity of the fluid (m^2 s^{-1})
ρ	fluid density (kg m^{-3})
μ	coefficient of viscosity of the fluid
σ	electrical conductivity
τ	shearing stress (N m^{-2})

subscripts

0	conditions at the stationary plate
1	conditions at the uniform motion plate

The principle of controlling the temperature of a heated body and the natural convection on a heated surface by suction of the fluid and heat transfer from the boundary layer to the wall finds its applications in several engineering situations of which a high temperature heat exchanger is one such instance. Mass transfer is used in flow problems in order to evaluate the distribution of species concentration and the corresponding species flux. It is well known that fluid particles may slip at the boundary of the surface, in certain situations of a geothermal region. Further, heat sinks find their use in engineering applications where the prime concern is to dissipate as much heat as possible from a heated surface within a short time.

Suction and injection at the plate also play a fundamental role in the plane Couette flow. It remains two-dimensional if the suction and injection applied at the porous parallel plate are uniform, but by the application of the transverse sinusoidal injection at the stationary plate and constant suction at the moving plate, the flow remains three-dimensional as studied by Singh [1]. A similar problem of three dimensional Couette flow of dusty viscous fluid was investigated by Govindarajan et al. [2] with transpiration cooling. Such flow problems are important for studies of transpiration cooling process by investigating associated heat transfer problems. Zaturska et al. [3] reported on the flow of viscous fluid driven along a channel by suction at porous walls. More recently, King and Cox [4] performed an asymptotic analysis of the steady-state and time-dependent laminar porous channel flows. Das et al. [5] studied the three dimensional Couette flow of a viscous incompressible electrically conducting fluid between two infinite horizontal parallel porous flat plates in presence of a transverse magnetic field. Sharma and Saini [6] investigated the effect of injection/suction between two horizontal parallel porous flat plates, with transverse sinusoidal injection of fluid at the stationary plate and its corresponding removal by periodic suction through the plate in motion, assuming the sinusoidal injection at the lower plate and its corresponding removal by the upper plate in motion. Makinde and Chinyoka [7] studied the unsteady flow and heat transfer of a dusty fluid between two parallel plates with an external uniform magnetic field is applied perpendicular to the plates with a Navier slip boundary condition. The governing non-linear partial differential equations are solved numerically using a semi-implicit finite difference scheme. A three-dimensional Couette flow through a porous medium with heat transfer has also been investigated by Ahmed [8]. Fasogbon [9] studied the simultaneous buoyancy force effects of thermal and species diffusion through a vertical irregular channel by using parameter perturbation technique. The study of heat and mass transfer on the free convective flow of a viscous incompressible fluid past an infinite vertical porous plate in presence of transverse sinusoidal suction velocity and a constant free stream velocity was presented by Ahmed [10]. Moreover, Ahmed and Liu [11] analyzed the effects of mixed convection and mass transfer of three-dimensional oscillatory flow of a viscous incompressible fluid past an infinite vertical porous plate in presence of transverse sinusoidal suction velocity oscillating with time and a constant free stream velocity. Recently, Ahmed and Zueco [12] investigated the effects of Hall current, magnetic field, rotation of the channel and suction–injection on the oscillatory free convective MHD flow in a rotating vertical porous channel when the entire system rotates about an axis normal to the channel plates and a strong magnetic field of uniform strength is

applied along the axis of rotation. Hossain and Rees [13] examined the effects of combined buoyancy forces from thermal mass diffusion by natural convection flow from a vertical wavy surface. Jain and Gupta [14] studied the effects of transverse sinusoidal injection velocity distribution on the free convective flow of a viscous incompressible fluid in slip flow regime under the influence of heat source. Chamkha et al. [15] presented an interesting study of the combined micropolar heat transfer and flow in a vertical channel. Such studies were confined to purely fluid regimes.

Chemically reacting fluids offer many technological applications ranging from the formation of thin films for electronics, combustion reactions, catalysis, biological systems, etc. ([8,16]). Couette flow geometry is one of the configurations used in industry, especially for polymer processing [17]. Ahmed and Chamkha [18] presented the effects of chemical reaction and conduction radiation on heat and mass transfer flow over a porous vertical plate with induced magnetic field. Couette flow can occur in between parallel plates, in a circular geometry, or in spherical geometry. Non-Newtonian fluids in Couette geometries have been extensively analyzed for different purposes. Ahmed and Joaquin [19] investigated the effect of the chemical reaction on a steady mixed convective heat and mass transfer flow of an incompressible viscous electrically conducting fluid past an infinite vertical isothermal porous plate taking into account the induced magnetic field, viscous and magnetic dissipations of energy. Ahmed [20] investigated the effects of chemical reaction on the transient MHD free convective flow in a slip flow regime. The porosity and magnetohydrodynamic effects on a horizontal channel flow of a viscous incompressible electrically conducting, Newtonian and radiating fluid through a porous medium in the presence of thermal radiation and transverse magnetic field were studied by Ahmed and Kalita [21]. Ahmed and Kalita [22] incorporated the model of magnetohydrodynamic transient convective radiative heat transfer in an isotropic, homogenous porous regime adjacent to a hot vertical plate using the Laplace transform method. The effects of conduction–radiation, porosity and chemical reaction on unsteady hydromagnetic free convection flow past an impulsively-started semi-infinite vertical plate embedded in a porous medium in the presence of first order chemical reaction and thermal radiation were analyzed by Ahmed [23] and the boundary layer equations are solved by an efficient, accurate, extensively validated and unconditionally stable finite difference scheme of the *Crank–Nicolson* type.

The aim of the present paper is to investigate MHD effects on a channel flow with heat and mass transfer in the presence of a chemical reaction of first order. In the present work, the effects of the physical flow parameters on the non-dimensional skin-friction components at the plates in the main flow and transverse directions, the dimensionless rates of heat and mass transfer at the plates, against the Reynolds's number have been presented. The behavior of the velocity field, temperature and concentration fields has been analyzed. In other words, the free convection heat and mass transfer effects on the aforementioned Couette flow in the slip flow regime in the presence of a uniform magnetic field and a heat sink has also been investigated.

2. Basic equations

Introducing a coordinate system (Fig. 1) with the plates oriented vertically parallel to the $\bar{x}$–$\bar{z}$ plane, such that the $\bar{x}$-axis

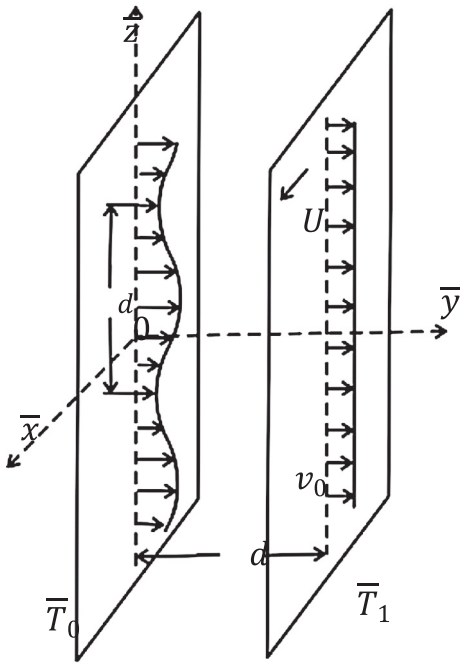

Figure 1 Couette flow with periodic injection and constant suction.

is oriented along the length of the plates in the direction of the buoyancy force and the $\bar{y}$-axis is perpendicular to the plane of the plates and directed into the fluid region. The plate at rest is subject to a transverse sinusoidal injection velocity distribution of the form

$$\bar{v} = v_0\left[1 + \varepsilon\cos\left(\frac{\pi\bar{z}}{d}\right)\right], \tag{1}$$

where $v_0 > 0$ and $0 \leqslant \varepsilon \ll 1$. Here v_0 is the undistributed part of the injection velocity, d is the wavelength of the periodic injection velocity and ε is a reference parameter. The outer plate has a uniform motion U in the $\bar{x}$-direction and is subjected to a constant suction, v_0 under first-order velocity slip conditions. Without loss of generality, the distance between the plates may be taken equal to the wavelength, d of the suction velocity. A uniform magnetic field is applied normal to the plane of the plates. The contributions of viscous and Joulean dissipation in the energy equation are small and can be neglected. This assumption has been shown to be applicable to a similar problem when no external electric field is imposed on the flow. All of the fluid properties are assumed to be independent of $\bar{x}$, except possibly the pressure. However, the flow remains three dimensional due to the form suction velocity distribution and the constant suction at the respective plates, as assumed above. Let $\overline{T}_0, \overline{C}_0$ be respectively the temperature and the molar species concentration of the fluid at the plate at rest. Further, let the temperature and molar species concentration at the plate in uniform motion are $\overline{T}_1, \overline{C}_1$, respectively. Let $\vec{q} = \bar{u}\hat{i} + \bar{v}\hat{j} + \bar{w}\hat{k}$ be the velocity vector of the fluid at the point $(\bar{x}, \bar{y}, \bar{z})$, where $\hat{i}, \hat{j}, \hat{k}$ are the unit vectors along the coordinate axes. Let $\vec{B} = B_0\hat{j}$ be the applied magnetic field, where B_0 is the magnetic field component along $\bar{y}$-axis. Let $\overline{T}, \overline{C}$ be respectively the temperature and molar species concentration

of the fluid. Let $\overline{T}_e, \overline{C}_e$ be respectively the equilibrium temperature and molar species concentration of the fluid. The magnetic Reynolds number is assumed to be small so that the induced magnetic field can be neglected. The level of species concentration in the fluid is very low so that the Soret and Dufour effects can be neglected.

The equations governing steady heat and mass transfer by natural convective motion of an incompressible viscous electrically conducting fluid through a vertical channel in presence of a magnetic field are given by

Equation of continuity

$$\frac{\partial \bar{v}}{\partial \bar{y}} + \frac{\partial \bar{w}}{\partial \bar{z}} = 0, \tag{2}$$

Equations of momentum

$$\bar{v}\frac{\partial \bar{u}}{\partial \bar{y}} + \bar{w}\frac{\partial \bar{u}}{\partial \bar{z}} = g\beta(\overline{T} - \overline{T}_e) + g\bar{\beta}(\overline{C} - \overline{C}_e) + \nu\left(\frac{\partial^2 \bar{u}}{\partial \bar{y}^2} + \frac{\partial^2 \bar{u}}{\partial \bar{z}^2}\right) - \frac{\sigma B_0^2 \bar{u}}{\rho}, \tag{3}$$

$$\bar{v}\frac{\partial \bar{v}}{\partial \bar{y}} + \bar{w}\frac{\partial \bar{v}}{\partial \bar{z}} = -\frac{1}{\rho}\frac{\partial \bar{p}}{\partial \bar{y}} + \nu\left(\frac{\partial^2 \bar{v}}{\partial \bar{y}^2} + \frac{\partial^2 \bar{v}}{\partial \bar{z}^2}\right), \tag{4}$$

$$\bar{v}\frac{\partial \bar{w}}{\partial \bar{y}} + \bar{w}\frac{\partial \bar{w}}{\partial \bar{z}} = -\frac{1}{\rho}\frac{\partial \bar{p}}{\partial \bar{z}} + \nu\left(\frac{\partial^2 \bar{w}}{\partial \bar{y}^2} + \frac{\partial^2 \bar{w}}{\partial \bar{z}^2}\right) - \frac{\sigma B_0^2 \bar{w}}{\rho}, \tag{5}$$

Equation of energy

$$\bar{v}\frac{\partial \overline{T}}{\partial \bar{y}} + \bar{w}\frac{\partial \overline{T}}{\partial \bar{z}} = \frac{\kappa}{\rho C_P}\left(\frac{\partial^2 \overline{T}}{\partial \bar{y}^2} + \frac{\partial^2 \overline{T}}{\partial \bar{z}^2}\right) + \frac{Q}{\rho C_P}(\overline{T} - \overline{T}_e), \tag{6}$$

Equation of mass diffusion

$$\bar{v}\frac{\partial \overline{C}}{\partial \bar{y}} + \bar{w}\frac{\partial \overline{C}}{\partial \bar{z}} = D\left(\frac{\partial^2 \overline{C}}{\partial \bar{y}^2} + \frac{\partial^2 \overline{C}}{\partial \bar{z}^2}\right) - \overline{K}(\overline{C} - \overline{C}_e). \tag{7}$$

The last term on the right hand side of Eq. (6) represents the heat absorption ($Q < 0$) or generation ($Q > 0$) varying directly with the temperature difference.

The corresponding boundary conditions are

$$\left\{\begin{array}{l} \bar{y} = 0 : \bar{u} = 0, \quad \bar{v} = v_0\left[1 + \varepsilon\cos\left(\frac{\pi\bar{z}}{d}\right)\right], \quad \bar{w} = 0, \quad \overline{T} = \overline{T}_0, \quad \overline{C} = \overline{C}_0 \\ \bar{y} = d : \bar{u} = U + L_1\frac{\partial \bar{u}}{\partial \bar{y}}, \quad \bar{v} = v_0, \bar{w} = 0, \quad \overline{T} = \overline{T}_1, \quad \overline{C} = \overline{C}_1 \end{array}\right\}, \tag{8}$$

where $L_1 = \left(\frac{2-m_1}{m_1}\right)L$, L is the mean free path and m_1 being the Maxwell's reflection coefficient.

Substituting the following non-dimensional quantities

$$y = \frac{\bar{y}}{d}, \quad z = \frac{\bar{z}}{d}, \quad p = \frac{\bar{p}}{\rho v_0^2}, \quad u = \frac{\bar{u}}{U}, \quad v = \frac{\bar{v}}{v_0}, \quad w = \frac{\bar{w}}{v_0},$$

$$Pr = \frac{\mu C_P}{\kappa}, \quad Sc = \frac{\nu}{D}, \quad h = \frac{L_1}{d},$$

$$Re = \frac{v_0 d}{\nu}, \quad M = \frac{\sigma B_0^2 d}{\rho v_0}, \quad \theta = \frac{\overline{T} - \overline{T}_e}{\overline{T}_0 - \overline{T}_e}, \quad \phi = \frac{\overline{C} - \overline{C}_e}{\overline{C}_0 - \overline{C}_e},$$

$$Gr = \frac{g\beta d(\overline{T}_0 - \overline{T}_e)}{U v_0}, \quad A = \frac{Q v d}{v_0 \kappa},$$

$$Gm = \frac{g\bar{\beta} d(\overline{C}_0 - \overline{C}_e)}{U v_0}, \quad m = \frac{(\overline{T}_1 - \overline{T}_e)}{(\overline{T}_0 - \overline{T}_e)}, \quad n = \frac{(\overline{C}_1 - \overline{C}_e)}{(\overline{C}_0 - \overline{C}_e)},$$

$$K = \frac{\overline{K} d}{v_0}.$$

into Eqs. (2)–(7) obtains the following non-dimensional equations

$$\frac{\partial v}{\partial y} + \frac{\partial w}{\partial z} = 0, \tag{9}$$

$$v\frac{\partial u}{\partial y} + w\frac{\partial u}{\partial z} = Gr\theta + Gm\phi + \frac{1}{Re}\left(\frac{\partial^2 u}{\partial y^2} + \frac{\partial^2 u}{\partial z^2}\right) - Mu, \tag{10}$$

$$v\frac{\partial v}{\partial y} + w\frac{\partial v}{\partial z} = -\frac{\partial p}{\partial y} + \frac{1}{Re}\left(\frac{\partial^2 v}{\partial y^2} + \frac{\partial^2 v}{\partial z^2}\right), \tag{11}$$

$$v\frac{\partial w}{\partial y} + w\frac{\partial w}{\partial z} = -\frac{\partial p}{\partial z} + \frac{1}{Re}\left(\frac{\partial^2 w}{\partial y^2} + \frac{\partial^2 w}{\partial z^2}\right) - Mw, \tag{12}$$

$$v\frac{\partial \theta}{\partial y} + w\frac{\partial \theta}{\partial z} = \frac{1}{PrRe}\left(\frac{\partial^2 \theta}{\partial y^2} + \frac{\partial^2 \theta}{\partial z^2}\right) + \frac{A\theta}{Pr}, \tag{13}$$

$$v\frac{\partial \phi}{\partial y} + w\frac{\partial \phi}{\partial z} = \frac{1}{Sc}\left(\frac{\partial^2 \phi}{\partial y^2} + \frac{\partial^2 \phi}{\partial z^2}\right) - K\phi. \tag{14}$$

The corresponding dimensionless boundary conditions become

$$\left\{\begin{array}{l} y = 0 : u = 0, \quad v = [1 + \varepsilon\cos(\pi z)], \quad w = 0, \quad \theta = 1, \quad \phi = 1 \\ y = 1 : u = 1 + h\frac{\partial u}{\partial y}, \quad v = 1, \quad w = 0, \quad \theta = m, \quad \phi = n \end{array}\right\}. \tag{15}$$

3. Method of solution

It is noted that, the amplitude ε of the injection is very small and hence, using a perturbation technique, the solution to this heat and mass transfer problem may be assumed to be of the following form

$$\left.\begin{array}{l} u(y,z) = u_0(y) + \varepsilon u_1(y,z) + \varepsilon^2 u_2(y,z) + \cdots, \\ v(y,z) = v_0(y) + \varepsilon v_1(y,z) + \varepsilon^2 v_2(y,z) + \cdots, \\ w(y,z) = w_0(y) + \varepsilon w_1(y,z) + \varepsilon^2 w_2(y,z) + \cdots, \\ p(y,z) = p_0(y) + \varepsilon p_1(y,z) + \varepsilon^2 p_2(y,z) + \cdots, \\ \theta(y,z) = \theta_0(y) + \varepsilon\theta_1(y,z) + \varepsilon^2\theta_2(y,z) + \cdots, \\ \phi(y,z) = \phi_0(y) + \varepsilon\phi_1(y,z) + \varepsilon^2\phi_2(y,z) + \cdots, \end{array}\right\} \tag{16}$$

When $\varepsilon = 0$, the problem reduces to a two-dimensional flow and is governed by the following equations obtained from Eqs. (9)–(14) using (16)

$$v_0' = 0, \tag{17}$$

$$u_0'' - Reu_0' - ReMu_0 + Re(Gr\theta_0 + Gm\phi_0) = 0, \tag{18}$$

$$p_0' = 0, \tag{19}$$

$$w_0'' - Rew_0' - ReMw_0 = 0, \tag{20}$$

$$\theta_0'' - PrRe\theta_0' + ARe\theta_0 = 0, \tag{21}$$

$$\phi_0'' - ScRe\phi_0' - ScReK\phi_0 = 0, \tag{22}$$

and the corresponding boundary conditions are

$$\left\{\begin{array}{l} y = 0 : u_0 = 0, \quad v_0 = 1, \quad w_0 = 0, \quad \theta_0 = 1, \quad \phi_0 = 1 \\ y = 1 : u_0 = 1 + hu_0', \quad v_0 = 1, \quad w_0 = 0, \quad \theta_0 = m, \quad \phi_0 = n \end{array}\right\}. \tag{23}$$

The solutions of Eqs. (17)–(22) subject to the boundary conditions (23) are

$$v_0 = 1, p_0 = constant, \quad w_0 = 0, \tag{24}$$

$$\theta_0(y) = C_1 e^{J_1 y} + C_2 e^{J_2 y}, \tag{25}$$

$$\phi_0(y) = C_3 e^{J_3 y} + C_4 e^{J_4 y}, \tag{26}$$

$$u_0(y) = C_5 e^{J_5 y} + C_6 e^{J_6 y} + C_7 e^{J_1 y} + C_8 e^{J_2 y} + C_9 e^{J_3 y} + C_{10} e^{J_4 y}. \tag{27}$$

The constants which are involved with Eqs. (24)–(27) have been presented in Appendix A.

When $\varepsilon \neq 0$, substituting (16) into Eqs. (9)–(14) and equating the coefficients of like powers of ε on both sides and neglecting higher order terms of ε^2, ε^3, etc., we obtain the following equations

$$\frac{\partial v_1}{\partial y} + \frac{\partial w_1}{\partial z} = 0, \tag{28}$$

$$\frac{\partial u_1}{\partial y} + v_1 \frac{\partial u_0}{\partial y} = \frac{1}{Re}\left(\frac{\partial^2 u_1}{\partial y^2} + \frac{\partial^2 u_1}{\partial z^2}\right) - (Gr\theta_1 + Gm\phi_1) - Mu_1, \tag{29}$$

$$\frac{\partial v_1}{\partial y} = -\frac{\partial p_1}{\partial y} + \frac{1}{Re}\left(\frac{\partial^2 v_1}{\partial y^2} + \frac{\partial^2 v_1}{\partial z^2}\right), \tag{30}$$

$$\frac{\partial w_1}{\partial y} = -\frac{\partial p_1}{\partial z} + \frac{1}{Re}\left(\frac{\partial^2 w_1}{\partial y^2} + \frac{\partial^2 w_1}{\partial z^2}\right) - Mw_1, \tag{31}$$

$$\frac{\partial \theta_1}{\partial y} + v_1 \frac{\partial \theta_0}{\partial y} = \frac{1}{PrRe}\left(\frac{\partial^2 \theta_1}{\partial y^2} + \frac{\partial^2 \theta_1}{\partial z^2}\right) + \frac{A\theta_1}{Pr}, \tag{32}$$

$$\frac{\partial \phi_1}{\partial y} + v_1 \frac{\partial \phi_0}{\partial y} = \frac{1}{ScRe}\left(\frac{\partial^2 \phi_1}{\partial y^2} + \frac{\partial^2 \phi_1}{\partial z^2}\right) - K\phi_1, \tag{33}$$

The corresponding boundary conditions for this case are

$$\left\{\begin{array}{l} y = 0 : u_1 = 0, \quad v_1 = \cos \pi z, \quad w_1 = 0, \quad \theta_1 = 0, \quad \phi_1 = 0 \\ y = 1 : u_1 = hu_1', \quad v_1 = 0, \quad w_1 = 0, \quad \theta_1 = 0, \quad \phi_1 = 0 \end{array}\right\}. \tag{34}$$

3.1. Cross flow solution

For the solution purpose, it is first assumed that Eqs. (28), (30) and (31) being independent of the main flow, temperature and concentration fields. The solutions for v_1, w_1, p_1 are considered to be of the following form

$$v_1(y,z) = v_{11}(y)\cos \pi z, \quad w_1(y,z) = -\frac{1}{\pi} v_{11}'(y) \sin \pi z,$$
$$p_1(y,z) = p_{11}(y)\cos \pi z, \tag{35}$$

where $v_{11}'(y)$ denotes differentiation of $v_{11}(y)$ with respect to y. Expressions $v_1(y, z)$ and $w_1(y, z)$ have been chosen so that the equation of continuity (28) is satisfied. Substituting (35) into (30) and (31), leads to

$$v_{11}'' - Rev_{11}' - \pi^2 v_{11} = Rep_{11}', \tag{36}$$

$$v_{11}''' - Rev_{11}'' - (\pi^2 + ReM)v_{11}' = \pi^2 Rep_{11}. \tag{37}$$

Eliminating p_{11} from Eqs. (36) and (37) yields

$$v_{11}^{IV} - Rev_{11}''' - (2\pi^2 + ReM)v_{11}'' + \pi^2 Rev_{11}' + \pi^4 v_{11} = 0. \tag{38}$$

The corresponding boundary conditions become

$$\left\{\begin{array}{l} y = 0 : v_{11} = 1, \quad v_{11}' = 0 \\ y = 1 : v_{11} = 0, \quad v_{11}' = 0 \end{array}\right\}. \tag{39}$$

3.2. Solutions for the main flow, temperature and the concentration fields

The solutions to Eqs. (29), (32) and 33) may be assumed u_1, θ_1, ϕ_1 as

$$u_1(y,z) = u_{11}(y)\cos \pi z, \quad \theta_1(y,z) = \theta_{11}(y)\cos \pi z,$$
$$\phi_1(y,z) = \phi_{11}(y)\cos \pi z. \tag{40}$$

Substituting Eq. (40) into Eqs. (29), (32) and (33), the following ordinary differential equations are obtained

$$u_{11}'' - Reu_{11}' - (\pi^2 + ReM)u_{11} + Reu_0'v_{11} + Re(Gr\theta_{11} + Gm\phi_{11})p_{11}' = 0, \tag{41}$$

$$\theta_{11}'' - PrRe\theta_{11}' + (ARe - \pi^2)\theta_{11} - PrRe\theta_0'v_{11} = 0, \tag{42}$$

$$\phi_{11}'' - ScRe\theta_{11}' + (KScRe + \pi^2)\phi_{11} - ScRe\phi_0'v_{11} = 0. \tag{43}$$

The corresponding boundary conditions are

$$\left\{\begin{array}{l} y = 0 : u_{11} = 1, \quad \theta_{11} = 0, \quad \phi_{11} = 0 \\ y = 1 : u_{11} = hu_1', \quad \theta_{11} = 0, \quad \phi_{11} = 0 \end{array}\right\}. \tag{44}$$

The finite difference formulae of $v_{11}', v_{11}'', v_{11}'''$ and v_{11}^{IV} are given by

$$\left.\begin{array}{l} v_{11}'(i) = \frac{v_{11}(i+1) - v_{11}(i-1)}{2h}, \\ v_{11}''(i) = \frac{v_{11}(i+1) - 2v_{11}(i) + v_{11}(i-1)}{h^2}, \\ v_{11}'''(i) = \frac{v_{11}(i+2) - 2v_{11}(i+1) + 2v_{11}(i-1) - v_{11}(i-2)}{2h^3}, \\ v_{11}^{\mathrm{IV}}(i) = \frac{v_{11}(i+2) - 4v_{11}(i+1) + 6v_{11}(i) - 4v_{11}(i-1) + v_{11}(i-2)}{h^4}. \end{array}\right\} \tag{45}$$

Substituting the finite difference formulae (44) into Eqs. (38), (41)–(43) gives the following equations

$$A_1 v_{11}(i+2) - A_2 v_{11}(i+1) + A_3 v_{11}(i) - A_4 v_{11}(i-1) + A_5 v_{11}(i-2) = 0, \tag{46}$$

$$A_1 u_{11}(i+1) - B_1 u_{11}(i) + A_5 u_{11}(i-1) = B(i), \tag{47}$$

$$H_1 \theta_{11}(i+1) - H_2 \theta_{11}(i) + H_3 \theta_{11}(i-1) = H(i), \tag{48}$$

$$E_1 \phi_{11}(i+1) - E_2 \phi_{11}(i) + E_3 \phi_{11}(i-1) = E(i). \tag{49}$$

All of the constants which appear in Eqs. (46)–(49) are presented in Appendix A.

3.3. Skin-friction coefficients

The non-dimensional skin-friction coefficients in the main flow direction at the plates ($y = 0, 1$) are given by

$$\tau_{x0} = \left(\frac{\partial u}{\partial y}\right)_{y=0} = u_0'(0) + \varepsilon u_{11}'(0)\cos \pi z, \tag{50}$$

$$\tau_{x1} = \left(\frac{\partial u}{\partial y}\right)_{y=1} = u_0'(1) + \varepsilon u_{11}'(1)\cos \pi z. \tag{51}$$

In addition, the non-dimensional skin friction coefficients in the transverse directions at the plates ($y = 0, 1$) are given by

$$\tau_{z0} = \left(\frac{\partial w}{\partial y}\right)_{y=0} = -\frac{\varepsilon}{\pi} v_{11}''(0)\sin \pi z, \tag{52}$$

$$\tau_{z1} = \left(\frac{\partial w}{\partial y}\right)_{y=1} = -\frac{\varepsilon}{\pi} v_{11}''(1)\sin \pi z. \tag{53}$$

3.4. Rate of heat transfer

The non-dimensional heat flux at the plates ($y = 0, 1$) in terms of the Nusselt numbers is given by

$$Nu_0 = \left(\frac{\partial\theta}{\partial y}\right)_{y=0} = \theta'_0(0) + \varepsilon\theta'_{11}(0)\cos\pi z, \tag{54}$$

$$Nu_1 = \left(\frac{\partial\theta}{\partial y}\right)_{y=1} = \theta'_0(1) + \varepsilon\theta'_{11}(1)\cos\pi z. \tag{55}$$

3.5. Rate of mass transfer

The non-dimensional mass flux at the plates ($y = 0, 1$) in terms of the Sherwood numbers is given by

$$Sh_0 = \left(\frac{\partial\phi}{\partial y}\right)_{y=0} = \phi'_0(0) + \varepsilon\phi'_{11}(0)\cos\pi z, \tag{56}$$

$$Sh_1 = \left(\frac{\partial\phi}{\partial y}\right)_{y=1} = \phi'_0(1) + \varepsilon\phi'_{11}(1)\cos\pi z. \tag{57}$$

3.6. Stability

Eqs. (46)–(57) have been solved by the Gauss–Seidel iteration method with the help of *FORTRAN* programming to obtain the velocity, temperature and concentration fields under the effect of different flow parameters. To prove convergence of the finite difference scheme, the computation was carried out for slightly changed value of 'h' by running the same program. No significant changes were observed in the values of $u, w, \theta$and ϕ and also after each cycle of iteration, the convergence check was performed. The convergence criterion tolerance was set as 10^{-8} which was satisfied at all points. Thus, it is concluded that the employed finite difference scheme is convergent and stable.

3.7. Accuracy

In order to check the accuracy of the employed numerical method, comparisons with the previously published work of Jain and Gupta [14] are performed. Tables 1 and 2 show comparisons of the present results for the crossflow velocity w and the fluid temperature θ for various Reynolds numbers and $Gm = K = 0$ with those of Jain and Gupta [14], respectively. It is clearly seen from Tables 1 and 2 that the results are in excellent agreement. These favorable comparisons with the work of Jain and Gupta [14] lend confidence in the numerical results to be reported subsequently.

Table 1 Comparison of the present results with the results of Jain and Gupta [14] for the crossvelocity w when $\varepsilon = 0.005$, $z = 0.3$, $Gr = 10, h = 0.2, m = 2 = n, Pr = 0.71, A = -1.5$, $Sc = 0.78$.

Y	Resent work		Jain and Gupta [14]	
	$Re = 0.5$	$Re = 1.0$	$Re = 0.5$	$Re = 1.0$
0.0	0.00000000	0.00000000	0.00000000	0.00000000
0.2	0.00361143	0.00318550	0.00357005	0.00315418
0.4	0.00460571	0.00435311	0.00458371	0.00433097
0.6	0.00367247	0.00387362	0.00364122	0.00385914
0.8	0.00213583	0.00248731	0.00211735	0.00243852
1.0	0.00000000	0.00000000	0.00000000	0.00000000

Table 2 Comparison of the present results with the results of Jain and Gupta [14] for the temperature profiles θ when $z = 0.3$, $Gr = 10, h = 0.2, m = 2 = n, Pr = 0.71, A = -1.5$, $Sc = 0.78$.

Y	Resent work		Jain and Gupta [14]	
	$Re = 0.5$	$Re = 1.0$	$Re = 0.5$	$Re = 1.0$
0.0	1.00000000	1.00000000	1.00000000	1.00000000
0.2	1.05879813	1.17098730	1.05669051	1.17063872
0.4	1.13560811	1.35153942	1.13450763	1.35009674
0.6	1.32725480	1.54757003	1.32580471	1.54539725
0.8	1.59650952	1.76984801	1.59473227	1.76730224
1.0	2.00000000	2.00000000	2.00000000	2.00000000

4. Results and discussion

Air has been considered for the medium of diffusion since it is electrically conducting. The Prandtl number for air at 298 K and 1 atmosphere is given by $Pr = 0.71$. It is also considered separately the gases: Hydrogen, Steam and Ammonia in ascending order of their Schmidt numbers are given by $Sc = 0.22, 0.60, 0.78$, respectively. Also kept ε and z fixed at $\varepsilon = 0.005$ and $z = 0.5$, unless otherwise stated. Further, the parameters $Gr = 10 = Gm, h = 0.5, m = 2, K = 2$ (endothermic reaction), and $A = -2$ were used for all of the following figures and tables.

Tables 3 and 4 depict the nature of crossflow velocity in y-direction (v) and crossflow velocity in z-direction (w) under the influence of Hartmann number and Reynolds number, respectively. From Tables 3 and 4 it is seen that v decreases throughout the channel as the fluid move from the plate at rest ($y = 0$) toward the plate in motion ($y = 1$). Further, in the regions of the channel close to the plate at rest it seems that v decreases with an increase in Hartmann number, but as the fluid move further out into the channel toward the plate in motion, it is seen that v increases as Hartmann number increases. In fact, v certainly increases with increasing values of Hartmann number in the regions close to the plate in motion. Also, it is seen that w initially increases from zero value (starting from the plate at rest) to some maximum value attainable at possibly

Table 3 Effects of M on v and w when $Re = 0.5$.

Y	v ($M = 5$)	v ($M = 10$)	w ($M = 5$)	w ($M = 10$)
0	1.0126558	1.0126558	0	0
0.2	1.0121892	1.0121729	0.0091756	0.0091573
0.4	1.0100774	1.0100157	0.0097527	0.0095594
0.6	1.0005271	1.0005875	0.0077594	0.0076332
0.8	1.0001783	1.0001995	0.0058119	0.0059071
1.0	1.0000000	1.0000000	0	0

Table 4 Effects of Re on v and w when $M = 5$.

Y	v ($Re = 0.5$)	v ($Re = 1$)	w ($Re = 0.5$)	w ($Re = 1$)
0	1.0126558	1.0126558	0	0
0.2	1.0121892	1.0125891	0.0091756	0.0085477
0.4	1.0100774	1.0103584	0.0097527	0.0094173
0.6	1.0005271	1.0005051	0.0077594	0.0078252
0.8	1.0001783	1.0003544	0.0058119	0.0061043
1.0	1.0000000	1.0000000	0	0

the middle of the channel and again decreases thereafter to zero value when one approaches the plate in motion. It is also observed that starting from the region very close to the plate at rest, w initially decreases with an increase in Hartmann number till about the middle of the channel and then increases thereafter with increasing values of Hartmann number when one gradually nears the plate in motion. It is obvious that in the regions of the channel close to the plate in motion, w increases with increasing values of Hartmann number. From Table 3, it is seen that v increases with an increase in Reynolds number, the regions of the channel given by $y \in (0, 1]$. Also, starting from the region very close to the plate at rest, w initially decreases with an increase in Reynolds number till about the middle of the channel and then increases again thereafter with increasing values of Reynolds number as one gradually approaches the plate in motion. Eventually, w increases with increasing values of Re in the regions of the channel close to the plate in motion. Also it has been see that the magnitude of v is greatest at the plate at rest and least at the plate in motion. This quite in agreement with the boundary conditions of the present problem. Also, $v > w$ within the considered range of values. It is also observed that the effects of M and Re on v are greatest at the plate at rest and are least at the plate in motion. Further, it is seen that the influence of Re and M on w is most significant at possibly the middle of the channel.

Fig. 2 shows the collective effects of the Hartmann number (M) Reynolds number (Re) and the chemical reaction parameter (K) on the main flow velocity (u) for conducting air ($Pr = 0.7$) in the case of plate cooling ($Gr > 0$) i.e. free convection currents convey heat away from the plate into the boundary layer. It is observed that an increase in the destructive chemical reaction parameter, K, from 0.2 through 0.5 to 1.0 produces a clear depression in the fluid velocity, i.e. the flow is decelerated up to the middle of the channel and after that a reverse trend is observed in the flow velocity with increasing values of chemical reaction. The influence of Hartmann number and Re on u profiles is therefore, expected to be strong. This is indeed the case as seen in Fig. 2. For constant Re ($= 0.5$), with a rise in the value of Hartmann number, from 2, 5 to 10 there is a strong reduction in velocity across the region $y \in [0, 0.6]$. A velocity peak arises close to the plate at rest for all profiles. The flow is therefore, decelerated with increasing values of the Hartmann number owing to the corresponding increase in the Lorentzian hydromagnetic drag force. Conversely, in the region $y \in [0.6, 1.0]$, with an increase in Hartmann number, there is a clear increase in the fluid velocity, i.e. the flow is accelerated. In the momentum Eqs. (10) and (12), the hydromagnetic terms, $-Mu$ and $-Mw$ deviate from classical magnetohydrodynamic flat-plate boundary layer flow owing to the presence of a negative magnetic term. The applied magnetic field, B_0, is therefore, effectively moving with the free stream. The resulting Lorentzian body force will therefore not act as a drag force as in conventional MHD flows, but as an aiding body force. This will serve to accelerate the flow and boost velocities in the channel near the plate in motion. Moreover, with constant Hartmann number value ($= 2.0$), as Reynolds number increases from 0.5 through 1.0 to 1.5, there is a distinct escalation in the fluid velocity across the region B_0, whereas a reverse trend is observed in the region $y \in [0.6, 1.0]$.

Fig. 3 shows the dimensionless temperature distribution (θ) with various magnetic parameters (M) and Reynolds number (Re). The trend is very consistent for all Hartmann and Reynolds number values such that the temperature decreases throughout the channel from a minimum at the plate at rest to the maximum $m = n = 2$ at the plate in motion. It is seen that the effects of Hartmann and Reynolds number on θ are least important near the plate at rest and most noteworthy near the plate in motion. Obviously, the temperature increases as y increases, under the influence of Hartmann and Reynolds number. An increase in the magnetic field strength and an increase in the relative effectiveness of inertia forces over viscous forces are desirable toward reducing the temperature in the channel.

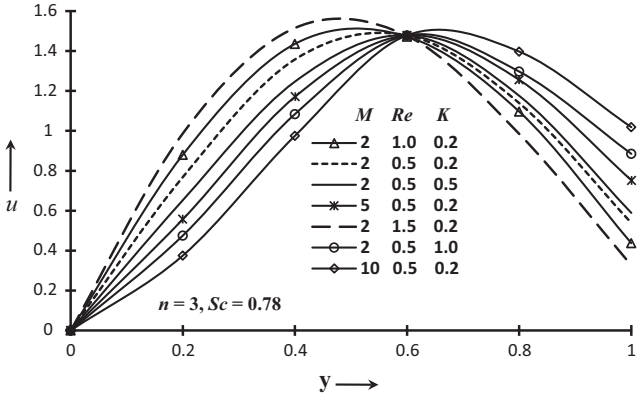

Figure 2 Main flow velocity profiles for different Hartmann, Reynolds and permeability numbers.

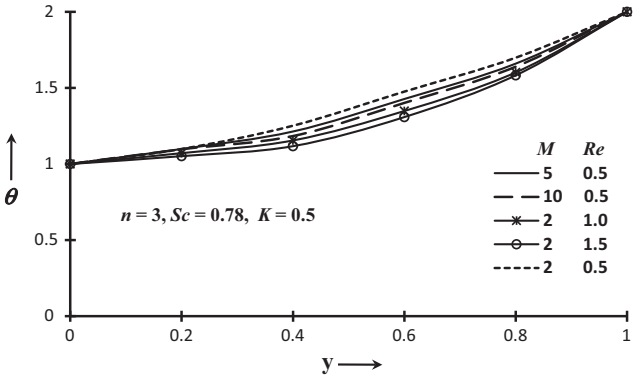

Figure 3 Temperature profiles for different Hartmann and Reynolds numbers.

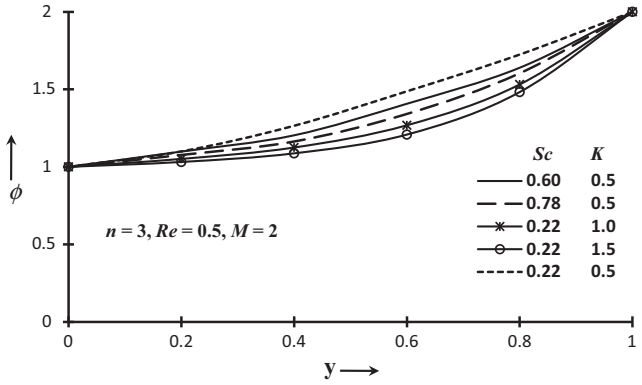

Figure 4 Concentration profiles for different Schmidt numbers and chemical reaction parameters.

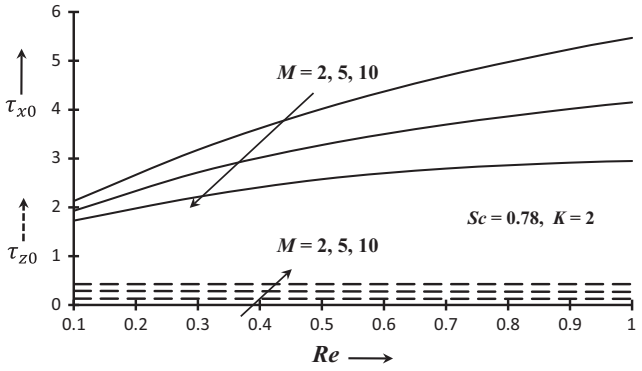

Figure 6 Skin-friction coefficients τ_{x0} and τ_{z0} for different Hartmann and Reynolds numbers.

Fig. 4 presents the species concentration profiles for various values of the Schmidt number (Sc) and endothermic chemical reaction parameter (K). The Schmidt number quantifies the relative effectiveness of momentum and mass transport by diffusion. A higher value of Schmidt number amounts to a fall in the chemical molecular diffusivity, i.e. less diffusion therefore takes place by species transfer. An increase in Schmidt number or chemical reaction parameter suppresses the species concentration in the boundary layer regime. A higher value of Sc implies a decrease of the molecular diffusivity causing a reduction in the concentration boundary layer thickness. On the other hand, a lower value of Schmidt number results in higher concentrations, i.e. greater molecular (species) diffusivity, causes an increase in the concentration boundary layer thickness. The effect of Schmidt number or chemical reaction parameter on ϕ is greatest near the plate in motion and least near the plate at rest.

From Fig. 5, it is seen that an increase in wall mass ratio (n) causes ϕ to increase in the regions of the channel given by $y \in [0, 1]$. Obviously, the molar species concentration field becomes equal throughout the channel when the molar species concentrations of the fluid at both the plates become equal. This is because mass flows from a region of higher concentration to a region of lower concentration. Thus, when the molar species concentrations of the fluid at both of the plates become equal, no more mass transfer takes place and hence, the molar species concentration field becomes equal (or rather uniform) all throughout the channel.

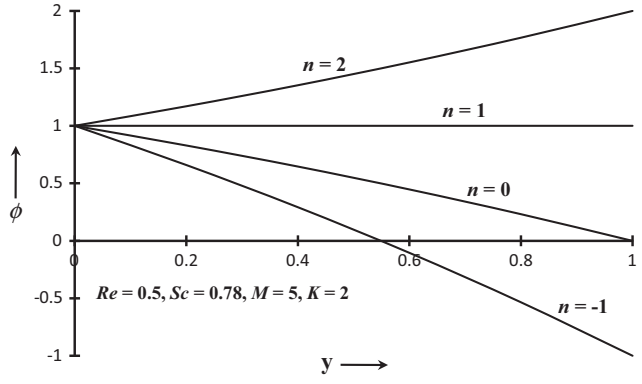

Figure 5 Concentration profiles for different wall-mass ratios.

Table 5 Effects of h and Re on u when $M = 5$.

Re	u ($h = 0$)	u ($h = 0.0001$)	u ($h = 0.01$)
0	0	0	0
0.2	0.9743952	0.9742891	0.9672561
0.4	1.5382174	1.5381584	1.5295227
0.6	1.8526271	1.8525177	1.8372594
0.8	1.9785344	1.9782541	1.9451312
1.0	1	1.0098427	1.0095782

Table 6 Effects of h and Re on τ_{x0} when $M = 7$.

Re	τ_{x0} ($h = 0$)	τ_{x0} ($h = 0.0001$)	τ_{x0} ($h = 0.01$)
0	1.9255782	1.9255758	1.9281528
0.2	2.9289732	2.9287329	2.9147526
0.4	3.9010751	3.9005572	3.8953327
0.6	4.6027917	4.6025725	4.5725931
0.8	5.1798361	5.1771935	5.0819317
1.0	5.3095273	5.3093817	5.3047172

Fig. 6 depicts the influence of the applied magnetic field on the non-dimensional coefficients of skin friction τ_{x0} and τ_{z0} at the plate at rest. The imposition of the magnetic field causes a decrease in the value of τ_{x0} whereas the value of τ_{z0} increases. It is noticed that the influence of either increasing the Reynolds number or increasing the magnetic field on the values of τ_{x0} is significant, whereas these effects on the values of τ_{z0} are insignificant.

Tables 5 and 6 present the nature of the main flow velocity (u) and the skin-friction coefficient τ_{x0} under the influence of the slip parameter (h). Within the considered range of values, it is to be noted that an increase in h causes u to decrease (provided $y > 0$) and τ_{x0} to decrease (provided $Re \in [0.3, 1]$). However, for $Re = 0.1$, we see that τ_{x0} increases as h increases. Obviously, when Re is too small, τ_{x0} should increase within an increase in h. Also, as the inertial forces and the viscous forces gradually become comparable with magnitude, we may say that τ_{x0} decreases with increasing values of h. Also, the value of u is greatest when $h = 0$ (provided $y > 0$). Further, when the inertial forces and the viscous forces are nearly equal in magnitude, it seems that τ_{x0} is greatest in the absence

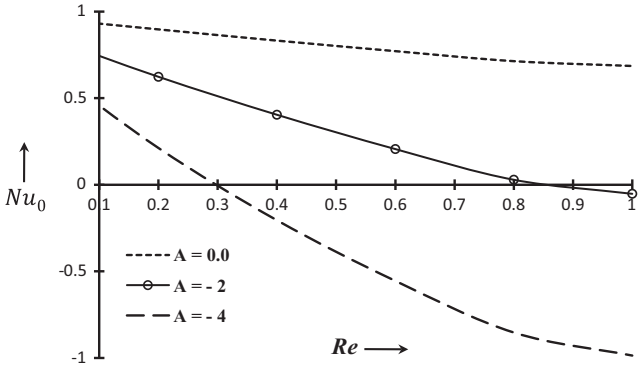

Figure 7 Wall heat flux Nu_0 at $y = 0$ for different heat sink parameters and Reynolds numbers.

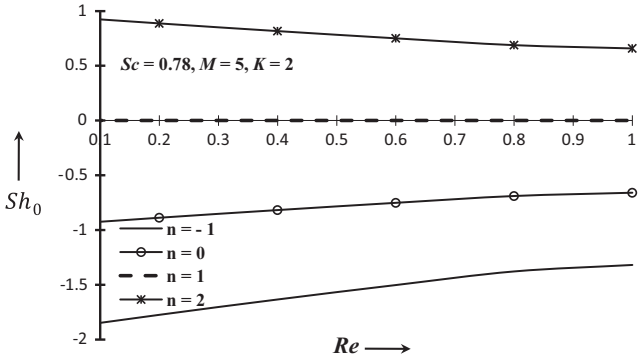

Figure 8 Wall mass flux Sh_0 at $y = 0$ for different wall-mass ratios and Reynolds numbers.

of slip. However, when the dominance of the viscous effects over the inertia effects is very large, it appears that τ_{x0} is least in the absence of slip. Also, for a given value of h, τ_{x0} increases with increasing values of Re and is maximum at $Re = 1$. Further, the effect of increasing h on τ_{x0} is insignificant when Re is small. It may be noted that for a given value of h, u first increases till possibly a little further than the middle of the channel and then starts decreasing thereafter, as one gradually nears the plate in motion. The effect of h on u assumes a greater significance near the plate in motion than near the plate at rest.

The effects of the heat sink parameter (A) and the Reynolds number (Re) on the wall heat flux Nu_0 at the plate $y = 0$ have been presented in Fig. 7 when $M = 5$ It is seen that an increase in the magnitude of the heat sink parameter causes Nu_0 to decrease as Re increases. In addition, it is also observed that the influence of heat sink on Nu_0 is insignificant for small values of Reynolds number. However, the effect of heat sink on Nu_0 assumes significance when the inertial forces are of nearly comparable magnitudes. For a given value of heat sink and increasing values of Reynolds number, Nu_0 decreases. On the other hand, Nu_0 values are greatest in the absence of a heat sink.

Fig. 8 demonstrates the behavior of the wall mass flux Sh_0 under the effects of wall mass ration (n) and Reynolds number (Re). It is seen that an increase in wall mass ration causes Sh_0 to decrease. Further, the effect of increasing wall mass ration on Sh_0 is most significant when Reynolds number is quite small ($Re = 0.1$) and least significant when Reynolds number is comparatively large ($Re = 1$). Again, it is noted that the rate of mass transfer at the plate $y = 0$ is zero i.e. when the molar species concentrations of the fluid at both plates become equal. However, for $Sc = 0.78$ and $n > 1$, Sh_0, decreases with increasing values of Reynolds number. Also, for $n < 1$, Sh_0, increases with increasing values of Reynolds number.

5. Conclusions

A mathematical model was presented for hydromagnetic three-dimensional Couette flow of a viscous, incompressible, electrically-conducting and chemically-reacting fluid between two vertical flat porous plates with a transverse sinusoidal injection of the fluid at the stationary plate and its corresponding removal by constant suction through the plate in uniform motion, with a chemical reaction first order. The governing non-linear coupled partial differential equations were solved by an implicit finite-difference scheme of Gauss–Seidel iteration technique and representative set of results were obtained to illustrate the details of flow characteristics and their dependence on some of the physical parameters. A comparison with previously published work was performed and the results were found to be in excellent agreement. On the basis of the above discussion it is concluded that with an increase in Hartmann number, the flow velocities u, v and w were decelerated near the plate $y = 0$, whereas a reverse trend was observed near the plate $y = 1$. Increasing Hartmann number and Reynolds number values decreased the temperature throughout the channel. The values of the fluid temperature were reduced considerably as either of the chemical reaction parameter or the Schmidt number was increased. Moreover, it was found that increasing either the slip parameter or the Reynolds number caused reductions in the skin-friction coefficients at the plate $y = 0$. In addition, it is concluded that the heat flux rate at the plate at $y = 0$ decreased as either of the heat sink parameter of the Reynolds number increased. Furthermore, the mass flux at the plate at $y = 0$ was predicted to decrease as the wall mass ratio increased. However, it increased as the Reynolds number increased for wall mass ratios less than unity while it decreased for wall mass ratios greater than unity.

Appendix A

$$J_1 = \frac{1}{2}\left[PrRe + \sqrt{Pr^2Re^2 + 4ReA}\right],$$

$$J_2 = \frac{1}{2}\left[PrRe - \sqrt{Pr^2Re^2 + 4ReA}\right],$$

$$J_3 = \frac{1}{2}\left[ScRe + \sqrt{Sc^2Re^2 + 4ScReK}\right],$$

$$J_4 = \frac{1}{2}\left[ScRe - \sqrt{Sc^2Re^2 + 4ScReK}\right],$$

$$J_5 = \frac{1}{2}\left[Re + \sqrt{Re^2 + 4ReM}\right],$$

$$J_6 = \frac{1}{2}\left[Re - \sqrt{Re^2 + 4ReM}\right],$$

$$C_1 = \frac{m - e^{J_2}}{e^{J_1} - e^{J_2}}, \quad C_2 = \frac{e^{J_1} - m}{e^{J_1} - e^{J_2}},$$
$$C_3 = \frac{n - e^{J_4}}{e^{J_3} - e^{J_4}}, \quad C_4 = \frac{e^{J_3} - n}{e^{J_3} - e^{J_4}},$$

$$C_5 = \frac{N - L(hJ_6 - 1)e^{J_6}}{(hJ_5 - 1)e^{J_5} - (hJ_6 - 1)e^{J_6}},$$
$$C_6 = \frac{L(hJ_5 - 1)e^{J_5} - N}{(hJ_5 - 1)e^{J_5} - (hJ_6 - 1)e^{J_6}},$$

$$C_7 = \frac{-ReGrC_1}{J_1^2 - ReJ_1 - ReM}, \quad C_8 = \frac{-ReGrC_2}{J_2^2 - ReJ_2 - ReM},$$
$$C_9 = \frac{-ReGmC_3}{J_3^2 - ReJ_3 - ReM},$$

$$C_{10} = \frac{-ReGmC_4}{J_4^2 - ReJ_4 - ReM}, \quad L = -(C_7 + C_8 + C_9 + C_{10}),$$

$$N = -1 + C_7(1 - hJ_1)e^{J_1} + C_8(1 - hJ_2)e^{J_2} + C_9(1 - hJ_3)e^{J_3} + C_{10}(1 - hJ_4)e^{J_4},$$

$$A_1 = 2 - hRe, \quad A_2 = 8 - 2hRe + 2h^2\left(2\pi^2 + MRe - \pi^2 h^3 Re\right),$$

$$A_3 = 12 + 4h^2(2\pi^2 + MRe) + 2\pi^4 h^4,$$
$$A_4 = 8 + 2hRe + 2h^2(2\pi^2 + MRe),$$

$$A_5 = 2 + hRe, \quad B_1 = 4 + 2h^2(2\pi^2 + MRe),$$

$$B(i) = -2Reh^2[v_{11}(i)B_2(i) + Gr\theta_{11}(i) + Gm\phi_{11}(i)],$$

$$B_2(i) = C_5J_5e^{J_5ih} + C_6J_6e^{J_6ih} + C_7J_1e^{J_1ih} + C_8J_2e^{J_2ih} + C_9J_3e^{J_3ih} + C_{10}J_4e^{J_4ih},$$

$$H_1 = 2 - hPrRe, \quad H_2 = 4 + 2h^2(\pi^2 - ARe),$$
$$H_3 = 2 + hPrRe,$$

$$H(i) = 2PrReh^2\left[C_1J_1e^{J_1ih} + C_2J_2e^{J_2ih}\right]v_{11}(i),$$

$$E_1 = 2 - hScRe, \quad E_2 = 4 + 2h^2\left(\pi^2 + KScRe\right),$$
$$E_3 = 2 + hScRe,$$

$$E(i) = 2ScReh^2\left[C_3J_3e^{J_3ih} + C_4J_4e^{J_4ih}\right]v_{11}(i).$$

References

[1] Singh KD. Three-dimensional Couette flow with transpiration cooling. J Appl Math Phys (ZAMP) 1999;50:661–8.

[2] Govindarajan A, Ramamurthy V, Sundarammal K. 3D Couette flow of dusty fluid with transpiration cooling. J Zhejiang Univ Sci A 2007;8(2):313–22.

[3] Zaturska MV, Drazin PG, Banks WHH. On the flow of a viscous fluid driven along a channel by suction at porous walls. Fluid Dyn Res 1998;4:151–78.

[4] King JR, Cox SM. Asymptotic analysis of the steady-state and time-dependent Berman problem. J Eng Math 2001;39:87–130.

[5] Das S, Mohanty S, Panda JP, Sahoo SK. Hydromagnetic three dimensional Couette flow and heat transfer. J Nav Archit Mar Eng 2008;5:1–10.

[6] Sharma PK, Saini BS. The effect of injection/suction on flow past parallel plates with transpiration cooling. Turk J Eng Environ Sci 2008;32:289–94.

[7] Makinde OD, Chinyoka T. MHD transient flows and heat transfer of dusty fluid in a channel with variable physical properties and Navier slip condition. Comput Math Appl 2010;60(3):660–9.

[8] Ahmed Sahin. Three-dimensional Channel flow through a porous medium. Bull Calcutta Math Soc 2009;101(5):503–14.

[9] Fasogbon PF. Analytical studies of heat and mass transfer by free convection in a two-dimensional irregular channel. Int J Appl Math Mech 2010;6:17–37.

[10] Ahmed S. The study of heat and mass transfer on free convective three-dimensional unsteady flows over a porous vertical plate. J Energy Heat Mass Transfer 2009;31:89–110.

[11] Ahmed S, Liu I-Chung. Mixed convective three-dimensional heat and mass transfer flow with transversely periodic suction velocity. Int J Appl Math Mech 2010;6:58–73.

[12] Ahmed S, Zueco J. Modelling of heat and mass transfer in a rotating vertical porous channel with Hall current. Chem Eng Commun 2011;198(10):1294–308.

[13] Hossain MA, Rees DAS. Combined heat and mass transfer in natural convection flow from a vertical wavy surface. Acta Mech 1999;136:133–41.

[14] Jain NC, Gupta P. Three dimensional free convection Couette flow with transpiration cooling. J Zhejiang Univ Sci A 2006;7(3):340–6.

[15] Chamkha AJ, Grosan T, Pop I. Fully developed combined convection of a micropolar fluid in a vertical channel. Int J Fluid Mech Res 2003;30:251–63.

[16] Chamkha AJ, Al-Mudhaf A, Al-Yatama J. Double-diffusive convective flow of a micropolar fluid over a vertical plate embedded in a porous medium with a chemical reaction. Int J Fluid Mech Res 2004;31:529–51.

[17] Chamkha AJ. MHD flow of a uniformly stretched vertical permeable surface in the presence of heat generation/absorption and a chemical reaction. Int Commun Heat Mass Transfer 2003;30:413–22.

[18] Ahmed S, Chamkha AJ. Effects of chemical reaction, heat and mass transfer and radiation on MHD flow along a vertical porous wall in the presence of induced magnetic field. Int J Ind Math 2010;2(4):245–61.

[19] Ahmed S, Zueco Joaquín. Combined heat and mass transfer by mixed convection MHD flow along a porous plate with chemical reaction in presence of heat source. Appl Math Mech 2010;31(10):1217–30.

[20] Ahmed S. Influence of chemical reaction on transient MHD free convective flow over a vertical plate in slip-flow regime. Emirates J Eng Res 2010;15(1):25–34.

[21] Ahmed S, Kalita K. A sinusoidal fluid injection/suction on MHD three-dimensional Couette flow through a porous medium in the

presence of thermal radiation. J Energy Heat Mass Transfer 2013;35:41–67.
[22] Ahmed S, Kalita K. Magnetohydrodynamic transient flow through a porous medium bounded by a hot vertical plate in presence of radiation: a theoretical analysis. J Eng Phys Thermophys 2013;86(1):31–9.
[23] Ahmed S. Numerical analysis for magnetohydrodynamic chemically reacting and radiating fluid past a non-isothermal impulsively started vertical surface adjacent to a porous regime. Ain Shams Eng 2014;5:923–33.

Sahin Ahmed, M.Sc., Ph.D., is presently working as an *Associate Professor and HoD* in the Department of Mathematics, *Rajiv Gandhi University*, Arunachal Pradesh, India. Before joining the University he served as an Assistant Professor in Goalpara College, Goalpara for more than eleven years. He obtained his M.Sc. Degree from the most glamorous *Delhi University*, Delhi and he has done his Ph.D. from Gauhati University, Guwahati. He started his research program career from the year 1998 and his research areas of interest are Computer oriented Heat and Mass transfer Fluid Dynamics and Magnetohydrodynamic Flows in porous media Transport. Active in research for over a decade, he has published over 75 journal papers in different internationally reputed peer reviewed journals to his credit in heat transfer, porous media flows, unsteady hydromechanics, rotating convection, heat transport in channel flow. Fifteen research scholars have obtained their *M. Phil degree's* and some research scholars have devoted their Ph.D. works under his supervision. He is currently dealing with few research projects sponsored by government of India. He regularly attends National and International Conferences/Workshops related to his research field. Presently he is working in modeling of *Mathematics Education and population study*.

Karabi Kalita, M.Sc., PGDCA, is a research scholar in the department of Mathematics, Gauhati University, Assam, India, under the supervision of Sahin Ahmed. She obtained her M.Sc. Degree from the oldest University of North East India, Gauhati University, Guwahati, Assam in the year 2011. She started her research pregame career from September 2011 and her research areas of interest are Fluid Dynamics and Magnetohydrodynamic Flows in porous media Transport. She has published Eight (8) research papers in different internationally reputed peer reviewed journals. She regularly attends National and International Conferences/Workshops related to her research field.

Ali J. Chamkha is Professor and Chairman of the Mechanical Engineering Department at the Prince Mohammad Bin Fahd University (PMU) in the Kingdom of Saudi Arabia. He earned his Ph.D. in Mechanical Engineering from Tennessee Technological University, USA, in 1989. His research interests include multiphase fluid-particle dynamics, fluid flow in porous media, heat and mass transfer, magnetohydrodynamics and fluid-particle separation. He has served as an Associate Editor for many journals such as International Journal of Numerical Method for Heat and Fluid Flow, Journal of Applied Fluid Mechanics, International Journal for Microscale and Nanoscale Thermal and Fluid Transport Phenomena and he is currently the Deputy Editor-in-Chief for the International Journal of Energy & Technology. He has authored and co-authored over 450 publications in archival journals and conferences.